

Electronic Supplementary Material (ESI) for Journal of Materials Chemistry A.
This journal is © The Royal Society of Chemistry 2022

Electronic Supplementary Information

In-situ formed copolymer electrolyte with high ionic conductivity and lithium-ion transference number for dendrite-free solid-state lithium metal batteries

Zhiheng Ren,[‡] Jixiao Li,[‡] Minghui Cai, Ruonan Yin, Jianneng Liang*, Qianling Zhang,
Chuanxin He, Xiantao Jiang, Xiangzhong Ren*

College of Chemistry and Environmental Engineering, Shenzhen University, Shenzhen,
Guangdong 518060, P.R. China

*Corresponding author:

Jianneng Liang, Email: jljan46@uwo.ca, Tel/Fax: +86-755-26558134

Xiangzhong Ren, Email: renxz@szu.edu.cn, Tel/Fax: +86-755-26558134

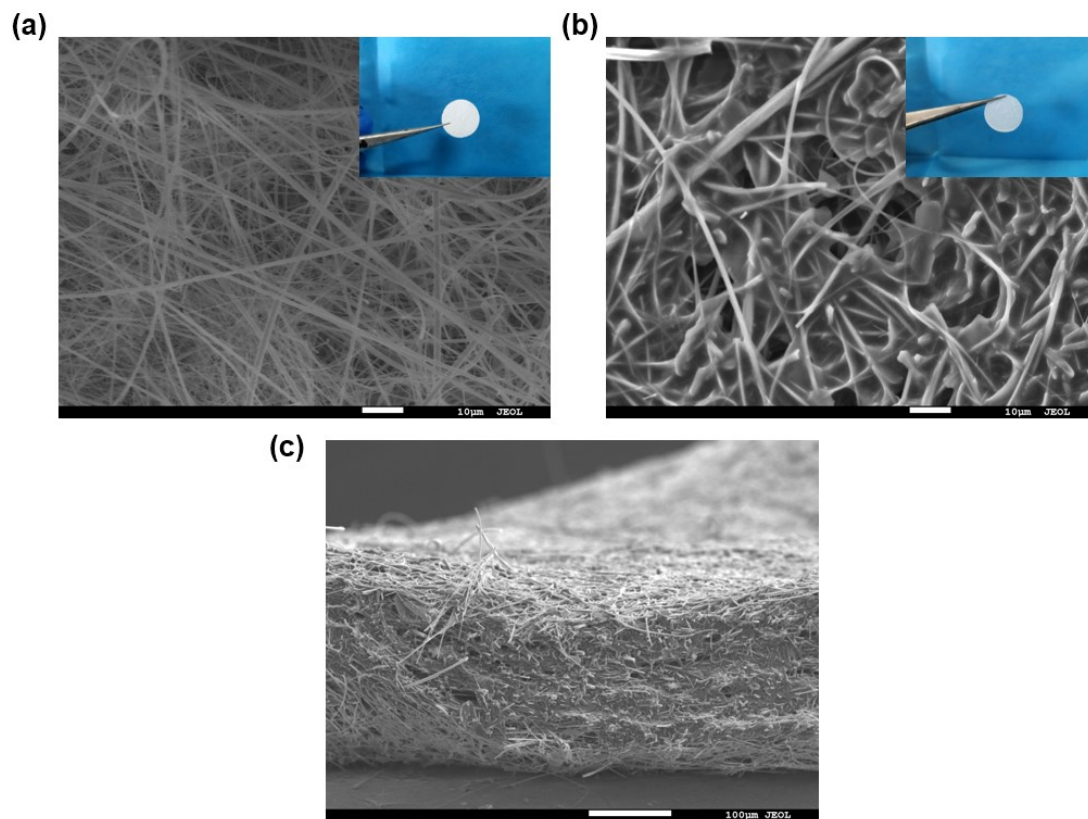


Fig. S1 SEM images of the top views of (a) pristine GF separator, (b) SN-CPE, the insets are the digital images, and (c) cross-sectional image of SN-CPE.

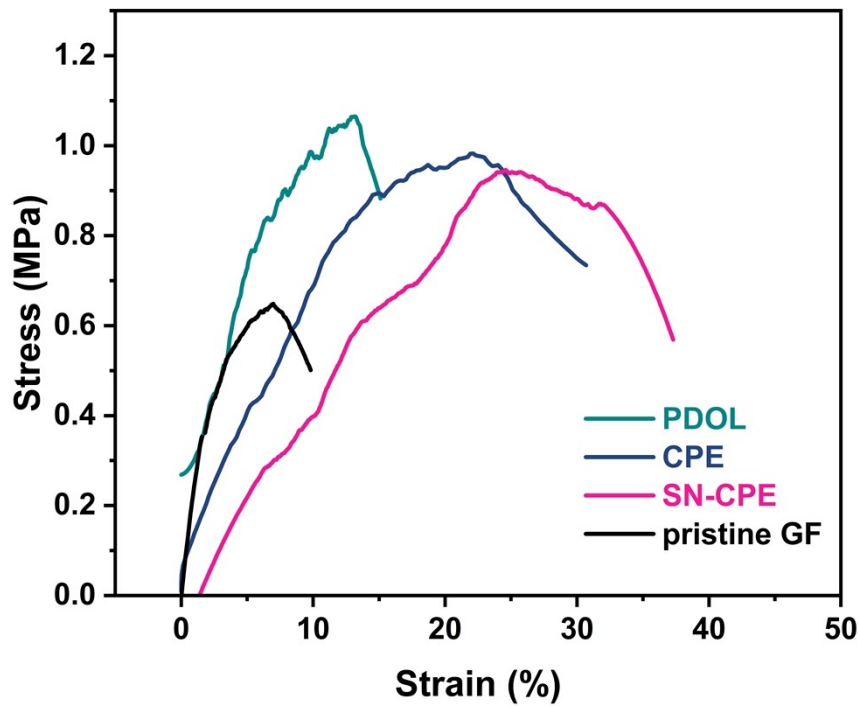


Fig. S2 Stress–strain curve of PDOL, CPE, SN-CPE and pristine GF membrane.

As shown in Fig. S2, all polymer electrolytes membranes exhibited higher fracture stress and break elongation compared to the pristine GF membrane due to the transformation of the liquid polymer electrolyte precursor into elastic quasi-solid PEs. In addition, SN-CPE and CPE exhibited higher break elongation due to DOL-TXE copolymer and the plasticization of SN, which is expected to be able to prevent lithium dendrite and improve the safety of batteries.

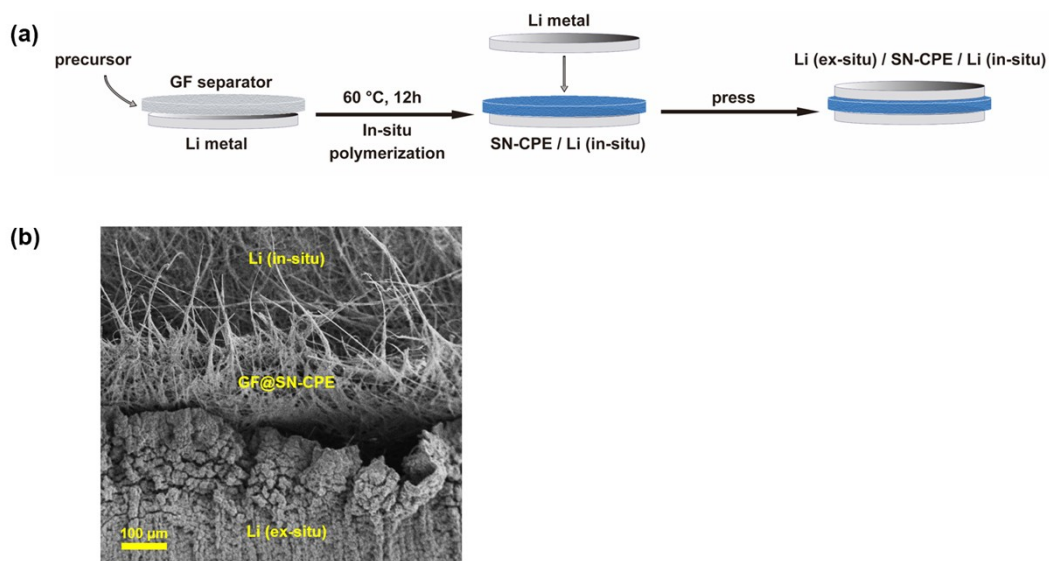


Fig. S3 (a) Schematic diagram for building Li (in-situ)/SN-CPE/Li (ex-situ) cell. (b) The cross-sectional SEM image of Li (in-situ) / SN-CPE interface (top), and SN-CPE / Li (ex-situ) interface (down).

As shown in Fig. S3a, the Li (in-situ)/SN-CPE/Li (ex-situ) cell was prepared by firstly putting the GF membrane on a Li metal foil, injecting the SN-CPE precursor in GF, and heating at 60°C for 12h for the polymerization reaction. After that, another piece of Li metal foil was placed on GF@SN-CPE membrane and pressurize them together to get a Li (in-situ) / SN-CPE / Li (ex-situ) cell. From the cross-section images, it can clearly find the poor contact between SN-CPE and Li (ex-situ). However, the interface between Li (in-situ) / SN-CPE is intimated.

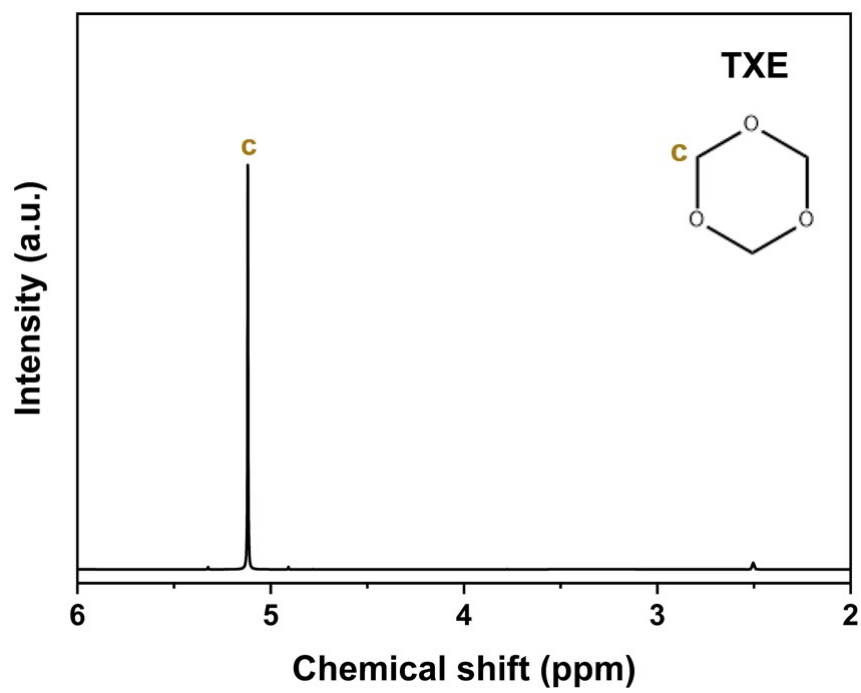


Fig. S4 ^1H NMR spectra of TXE.

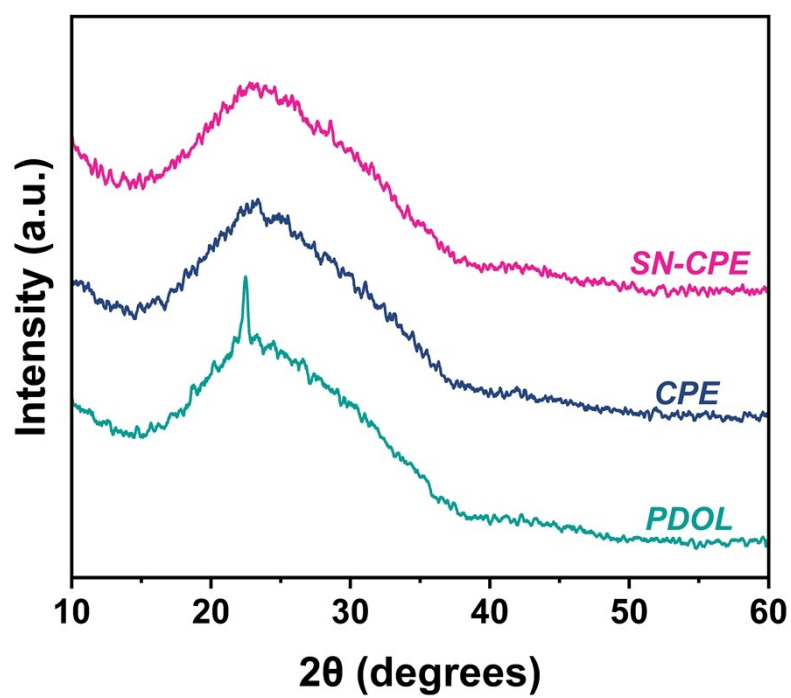


Fig. S5 XRD pattern of PDOL, CPE and SN-CPE.

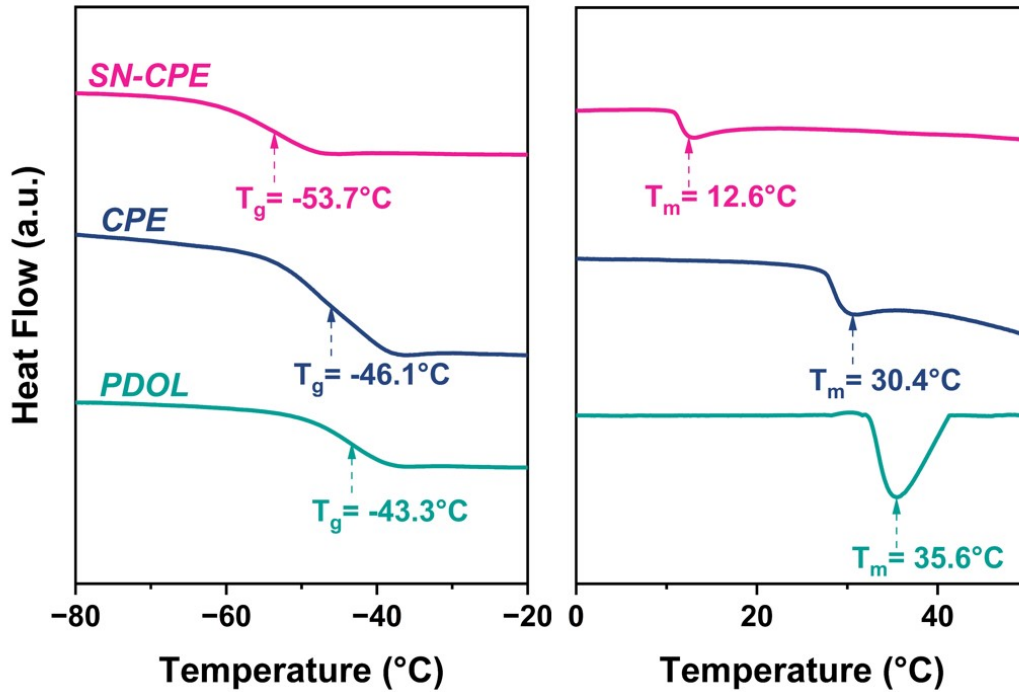


Fig. S6 DSC curves of PDOL, CPE and SN-CPE.

As shown in Fig. S6, the glass transition temperature (T_g) of PDOL is -43.3°C and the melting temperature (T_m) was 35.6°C . With the introduction of TXE, the T_g , T_m of CPE decreased slightly. After the addition of SN, a significant decrease of T_g , T_m to as low as -53.7°C and 12.6°C happened. The lower T_g temperature indicates that SN-CPE had faster polymer chain movement and Li^+ mobility. Besides, the T_m peak integration area of SN-CPE was significantly smaller than the other two PEs, indicating that SN-CPE was almost amorphous at working temperature.

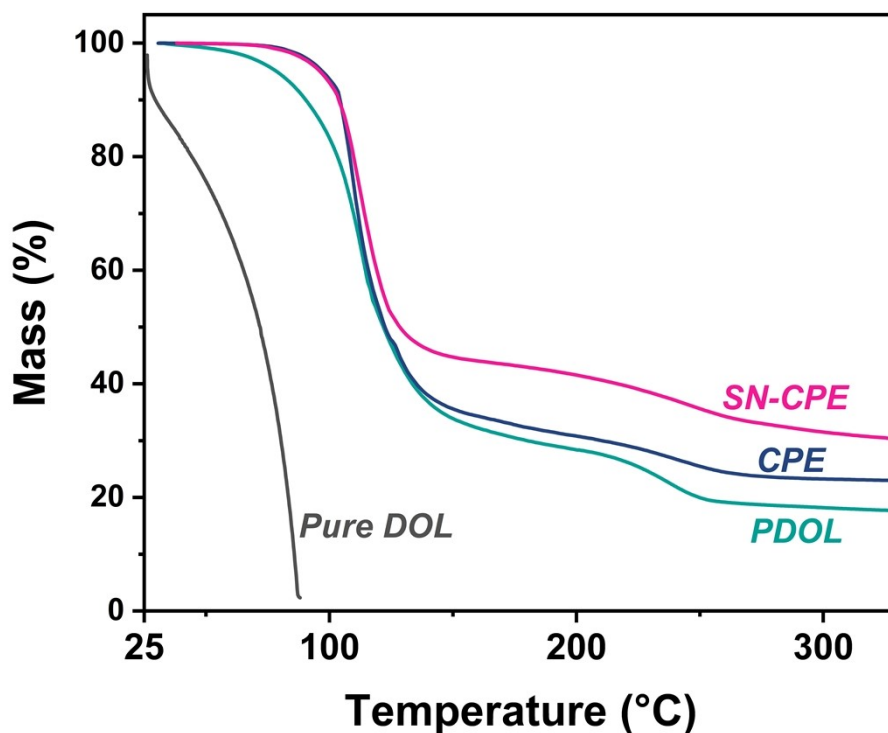


Fig. S7 TGA profiles of pure DOL, PDOL, CPE and SN-CPE.

Fig. S7 shows the thermogravimetric analysis (TGA) results of different PEs. TGA results suggest that SN-CPE and CPE had almost no weight loss in the temperature range from 25 to 80 °C, indicating their high safety performance. In addition, DOL is a low boiling point solvent and it can volatilize completely at 88°C. Therefore, the existence of DOL monomer will significantly reduce the thermal stability of the PE. It can be found that the copolymerization strategy will lead to an increase in the conversion of DOL monomer ring-opening reaction since there was almost not weight loss at the the temperature range from 25 to 90 °C for CPE and SN-CPE.

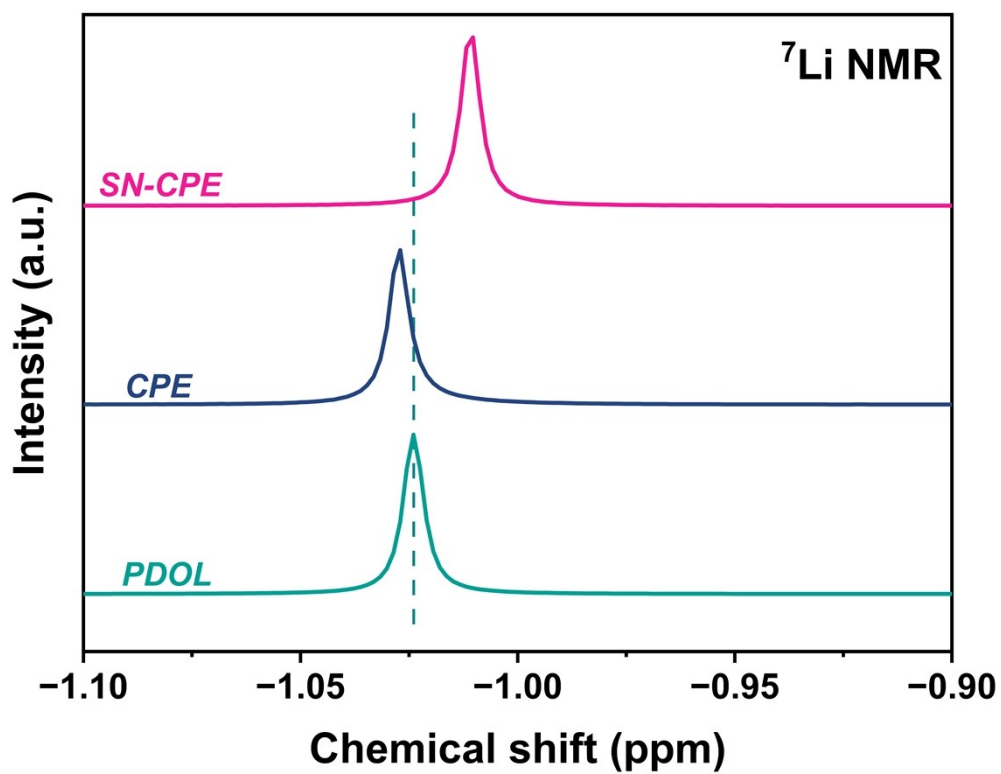


Fig. S8 ⁷Li NMR spectra of PDOL, CPE and SN-CPE.

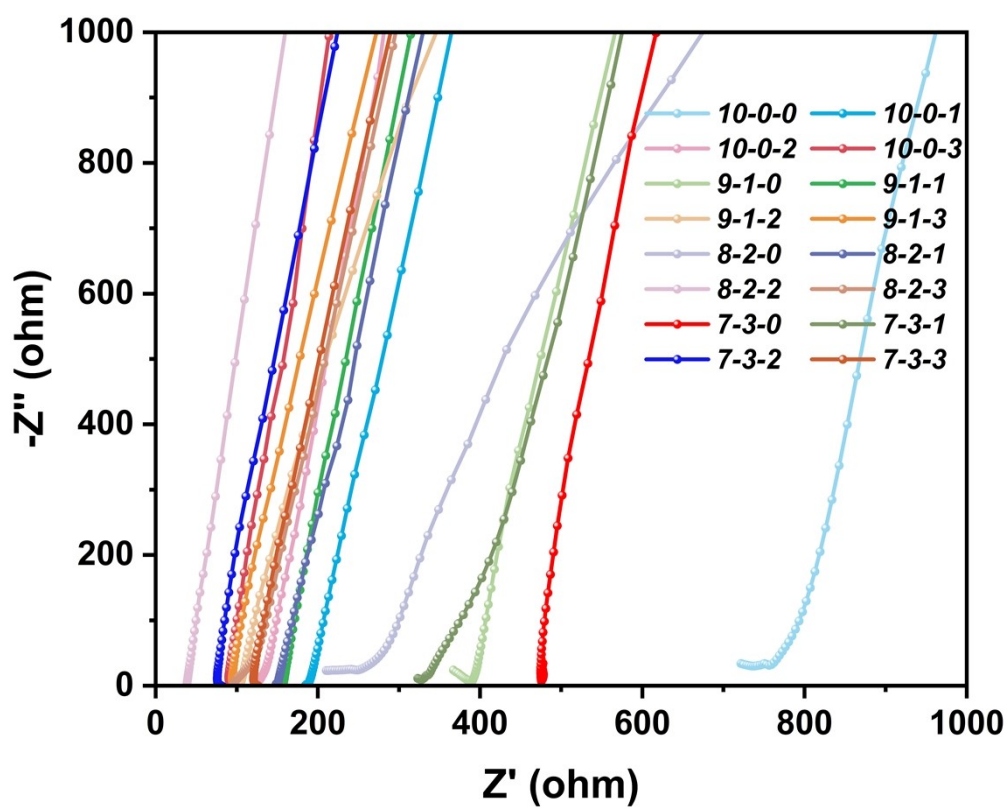


Fig. S9 Nyquist plots of PEs with different DOL:TXE:SN mass ratios at 25°C.

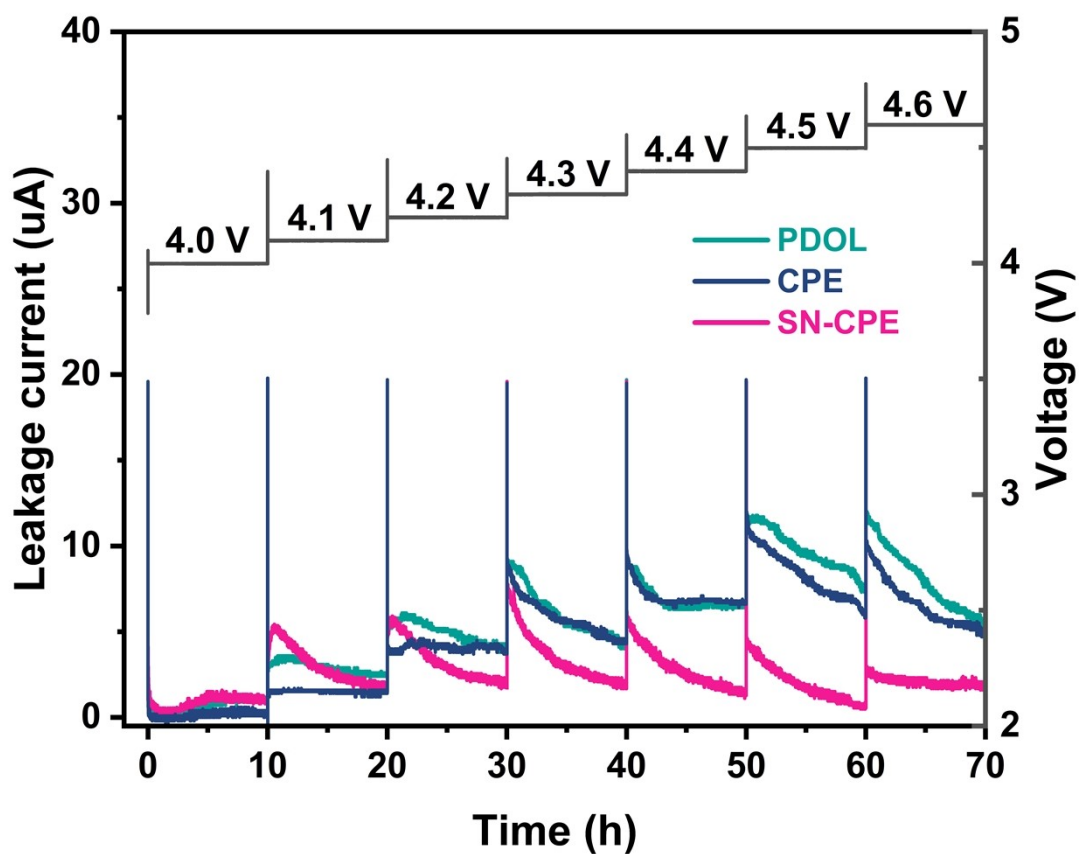


Fig. S10 Electrochemical floating test of PDOL, CPE and SN-CPE at 4.0 V to 4.6 V.

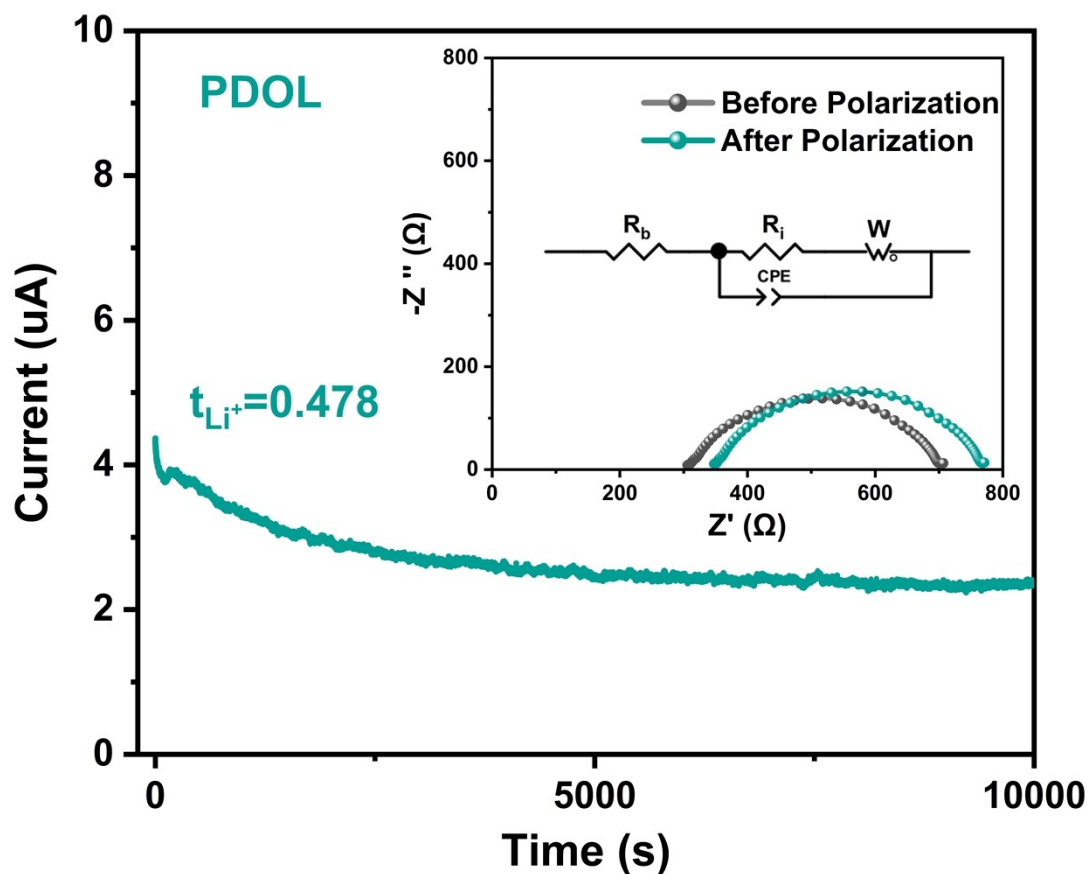


Fig. S11 Chronoamperometry curves with a step voltage of 10 mV (The insets displayed EIS plot before and after polarization) of PDOL.

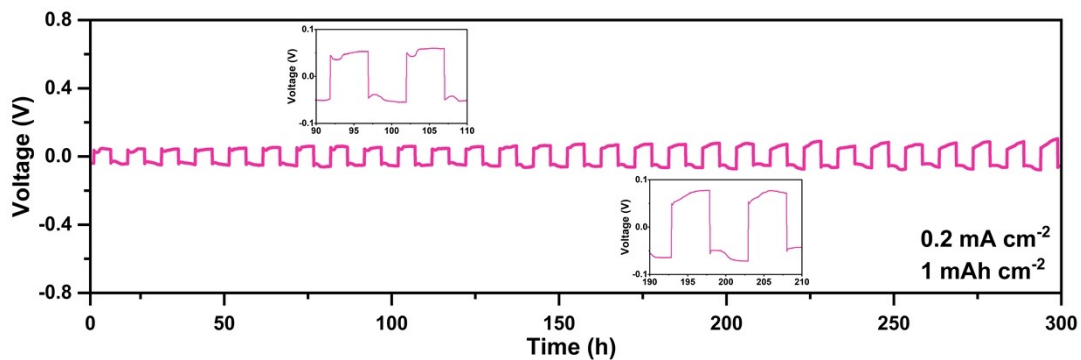


Fig. S12 Cycling performance of symmetric Li/Li cells with SN-CPE at 0.2 mA cm^{-2} and 1 mAh cm^{-2}

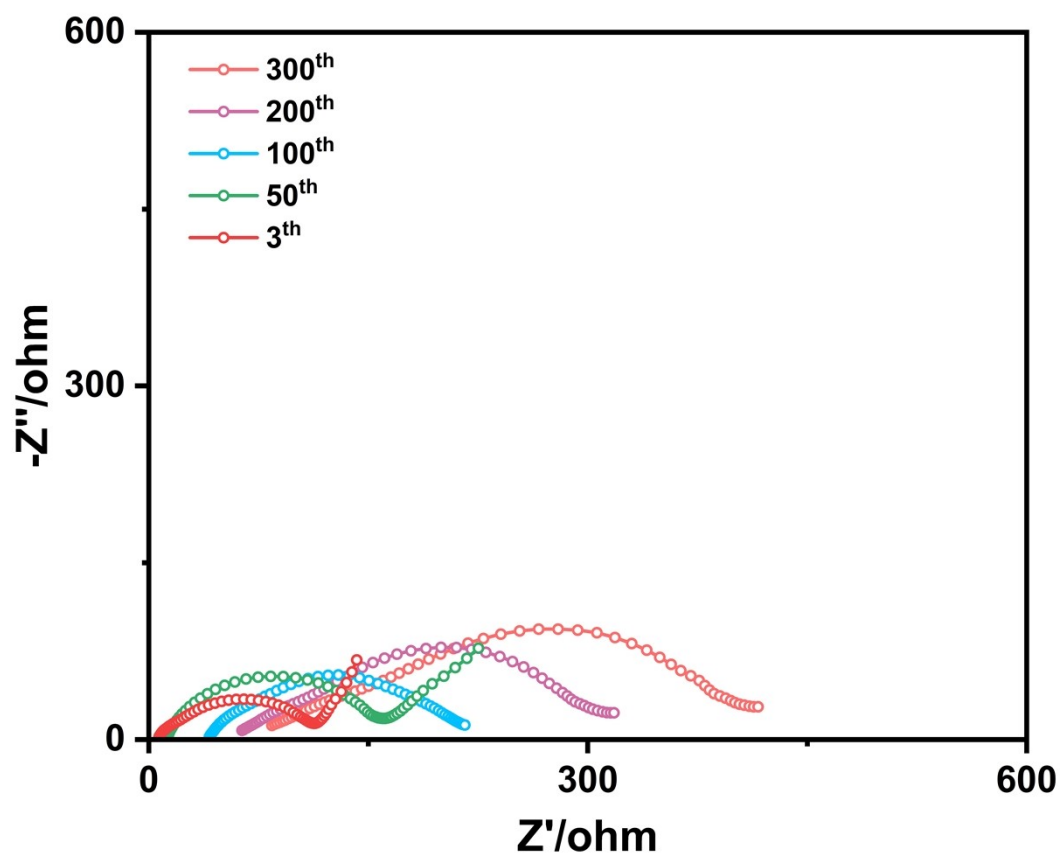


Fig. S13 The Nyquist plots of LFP | SN-CPE | Li cell at 1 C in different cycles.

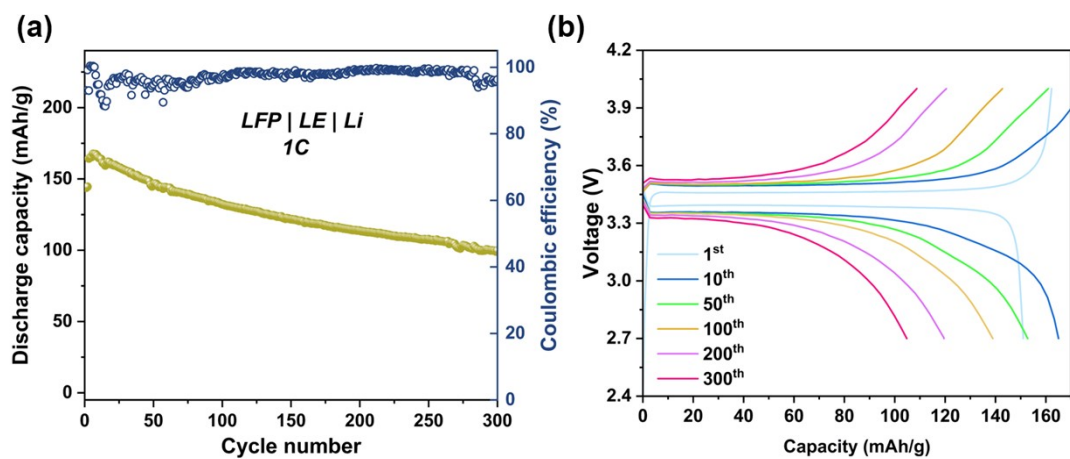


Fig. S14 Electrochemical performance of LFP | LE | Li cell at 1 C, 25 °C. (a) Cycling performance, (b) corresponding charge-discharge curves. LE means a liquid phase electrolyte with 2 M LiTFSI in DOL/DME solvent.

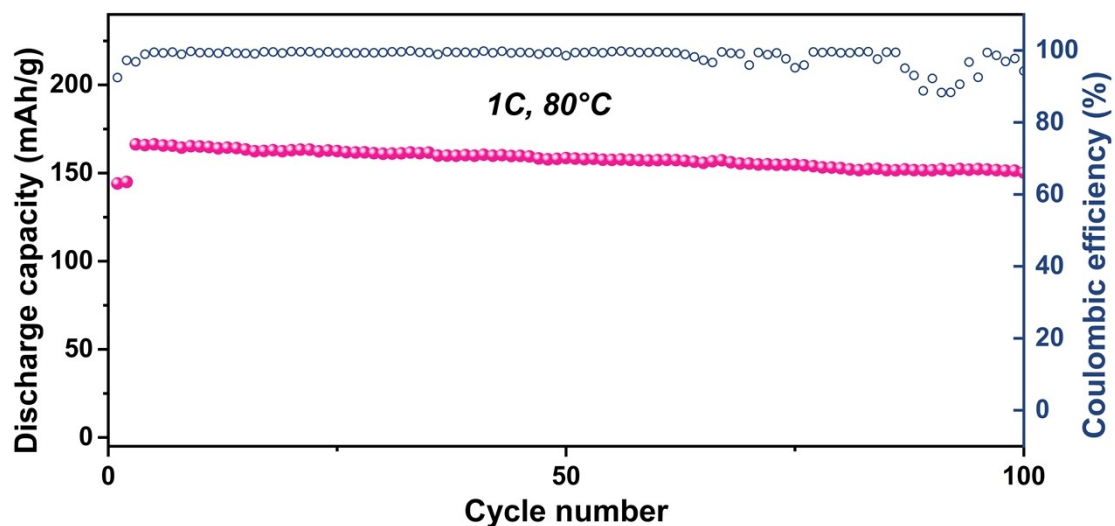


Fig. S15 Cycling performance of LFP | SN-CPE | Li cell at 1 C, 80 °C.

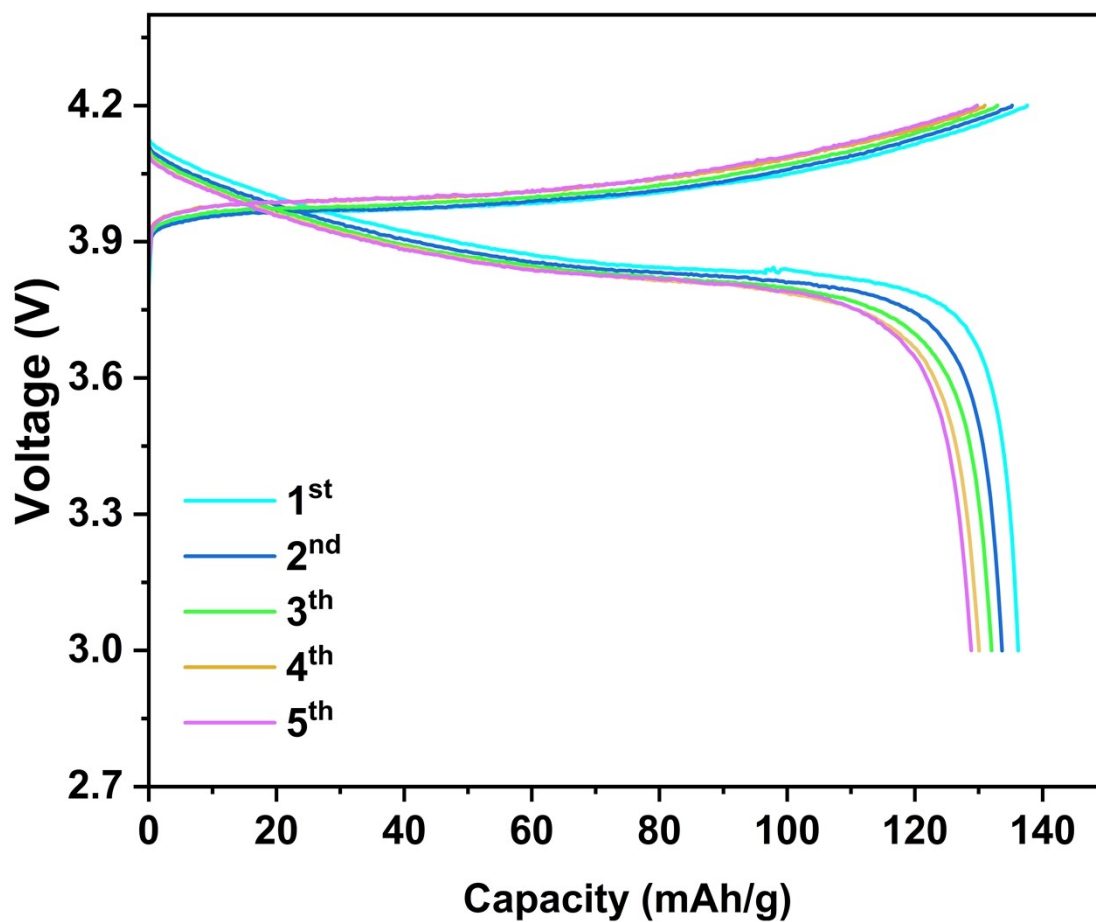


Fig. S16 Charge/discharge curves of the LiCoO₂ | SN-CPE | Li cell for the first 5 cycles at 0.2 C with a voltage of 3.0 to 4.2 V at 25 °C.

Table. S1 Gel permeation chromatography results of PEs

	M_n ^{a)}	M_w ^{b)}	PD ^{c)}
PDOL	3897	6975	1.78984
CPE	3095	5570	1.79968
SN-CPE	2686	4479	1.66754

a) number-averaged molecular weight, b) weight-averaged molecular weight, c) polydispersity index.

Table. S2 Changes of Binding energy (E_b , in eV) and Gibbs Free Energy of PDOL, P(DOL+TXE) and SN upon the interaction with free Li^+

	G (a.u)	ΔG (a.u)	E_b (eV)
Li	-7.28454		
PDOL	-884.904		
P(DOL-TXE)	-920.782		
SN	-264.305		
PDOL-Li	-892.25	-0.06237	-1.69723
P(DOL-TXE)-Li	-928.114	-0.04708	-1.28108
SN-Li	-271.655	-0.06562	-1.78574